



Tracing natural processes using isotopic abundances is probably the most successful aspect of modern geochemistry. The methods relying on isotopic data are analytically intensive since they depend on complex separation procedures and expensive equipment, but overall they are conceptually simple and robust. The natural variability of the abundances of isotopes in nature results from different processes:

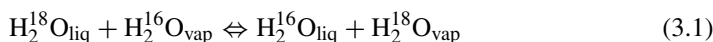
1. Under a variety of thermodynamic and kinetic conditions, isotopes distribute themselves unevenly among co-existing phases (minerals, liquids, gases). These effects are in general very subtle as are the differences between the isotopes that create them, which explains why they escaped detection until the 1950s.
2. Radioactivity removes the parent isotope from an element and adds the decay product to another: ^{87}Rb becomes ^{87}Sr . We will see in the next chapter that the rate of removal of the parent isotope is identical anywhere and at any time in the universe, so this process only affects the relative abundances of the radiogenic isotopes.
3. Cosmic rays are particles produced outside the Solar System and their origin is still not quite understood. The energy of some of these particles, mostly protons and α particles, occasionally exceeds the nuclear binding energy. In the upper atmosphere, some nuclei, such as nitrogen and oxygen, get chipped by the collision, a process known as “spallation.” Most particles reaching the ground are actually secondary and can be accounted for by spallation.
4. For all we should be concerned about at this point, the effect of nucleosynthetic processes stopped with the collapse of the solar nebula. We will see that some rare objects found in meteorites and known as refractory inclusions still keep the memory of a pre- or early-solar isotopic variability. Turbulence in the solar nebula and mixing upon planetary accretion and differentiation have for all practical purposes erased – with the remarkable exception of oxygen for which mass-independent fractionation among the Earth, the Moon, Mars, and the different groups of meteorites calls for different reservoirs – most traces of these heterogeneities in planetary bodies.

Thermodynamic modes of isotopic fractionation are collectively referred to as mass-dependent processes and are the topic of this chapter. Kinetic fractionation will be returned to in [Section 5.4](#). The logic underlying thermodynamic fractionation can be applied to isotopes with the added advantage that the behavior of two isotopes of the same element

will be more similar than that of two distinct elements, and, indeed, the chemistry of two isotopes of a heavy element, e.g. lead, is virtually unchanged. The applications of isotopic fractionation to the mapping of low- and medium-temperature phenomena are fundamental. The principles are rather similar to those set out in the previous chapter for chemical fractionation.

3.1 Principles of stable isotope fractionation

Let us imagine how isotopes ^{16}O ($\approx 99.8\%$ of natural oxygen) and ^{18}O are distributed between liquid water and vapor. The reaction can be written:



The four compounds appearing in this equation are chemically identical two by two, but differ by their isotopic abundances: they are known as isotopomers of H_2O . The mass action law governing this equilibrium is written:

$$\left(\frac{\text{H}_2^{18}\text{O}}{\text{H}_2^{16}\text{O}}\right)_{\text{vap}} / \left(\frac{\text{H}_2^{18}\text{O}}{\text{H}_2^{16}\text{O}}\right)_{\text{liq}} = \left(\frac{^{18}\text{O}}{^{16}\text{O}}\right)_{\text{vap}} / \left(\frac{^{18}\text{O}}{^{16}\text{O}}\right)_{\text{liq}} = \alpha_{\text{vap/liq}}^{\text{O}}(T, P) \quad (3.2)$$

The notation $\alpha_{\text{vap/liq}}^{\text{O}}(T, P)$ for the fractionation coefficient now replaces that of partition coefficients K to signal that the exchange concerns just a single nucleus. Fractionation coefficients are defined likewise for many stable isotope pairs, such as deuterium/hydrogen $^2\text{H}/^1\text{H}$ (D/H), $^{13}\text{C}/^{12}\text{C}$, $^{15}\text{N}/^{14}\text{N}$, $^{34}\text{S}/^{32}\text{S}$, etc., between such varied phases as gases, natural solutions, magmatic liquids, and minerals. The isotopes exchanged have the same outer electron configuration. Their chemical properties are therefore very similar and their molar volumes almost identical, making α very close to unity and virtually independent of pressure.

The Second Principle of Thermodynamics states that, because the stability of a system is only achieved when its energy is at its minimum, somewhere behind any fractionation factor looms a term that accounts for the exchange of energy between the different participants of a reaction. Before we set out to discuss the physics of stable isotope fractionation, let us therefore first summarize a few simple ideas about the different forms of internal energy in a system. Energy can be stored in different ways:

1. Translational energy. Even when a gas as a whole is at rest, its atoms and molecules move freely and therefore have a mean kinetic energy $\frac{1}{2}m\bar{v}^2$, where the bar indicates that the squared-velocity is averaged and m is the mass of the atom. Translational energy is the unique form of energy of monatomic species such as rare gases (He, Ne, etc.).
2. Rotational energy. Molecules have a momentum of inertia I which measures the mean squared-deviation of the mass from the main rotation axis and, for a given angular velocity ω , the rotational energy is $\frac{1}{2}I\omega^2$. Rotating charges, such as electrons, can be seen as little current loops, which act as little magnets, and the energy of the magnetic field is proportional to the magnetic moment.

3. Vibrational energy. Because they are subjected to combined attractive and repulsive forces, the individual atoms of a diatomic molecule, such as H and Cl in HCl, vibrate around their position at rest. The energy of this movement is the most important cause of isotopic fractionation. Acoustic waves in solids provide a collective form of vibrational energy. Vibrating charge pairs can be seen as little antennas. The energy that these antenna can emit or receive is proportional to the electric dipole of the pairs.
4. Electronic energy. Electrons in atoms and molecules can rise to energy levels above their ground state, normally from low-energy to high-energy orbitals by absorption of light. This phenomenon is, however, of very short duration and involves energies too large to be of concern in this chapter.

The total energy of a system is the sum of these four components. Vibrational and rotational energy are gained or lost by absorption or emission of photons, i.e. by interaction of matter with electromagnetic radiation, such as infrared, visible, or ultraviolet light. In much the same way as “kicks” (shocks) redistribute translational energy among gas molecules, the electromagnetic field carried by photons kicks the electronic dipole and magnetic moments. We are going to see that all these kicks must carry discrete amounts of energy.

Quantum mechanics states that energy is measured by quanta, that we can see as “grains,” which means that it is distributed over discrete energy levels. These quanta characterize the spacing between successive energy levels. For the conditions of temperature of interest to us, the translation quanta are much smaller than the rotational quanta, which themselves are much smaller than vibrational quanta (Fig. 3.1). The “classical” thermal energy RT (or kT for an isolated molecule with k being the Boltzmann constant) represents the equivalent of an enormous number of translational and rotational quanta, which indicates that the corresponding levels are well populated and can be treated as a continuum via the methods of classical physics. For reasons that will appear later, they do not produce temperature-dependent effects. At temperatures of geological interest, both translational and rotational energies are therefore unimportant for isotope fractionation in solids and liquids, with rare exceptions such as the CO_3 spinner of carbonate minerals. In contrast, the more energetic vibrational levels are more sparsely populated, which is the reason for the temperature dependence of isotopic effects, and they therefore will need special attention.

When two atoms come close to one another, their orbitals can interact with one another to form a single molecular orbital. The energy of a chemical bond, e.g. O–H for the hydroxyl radical, varies with the distance between the bonding atoms (Fig. 3.2). Although this plot does not describe the situation as accurately as true molecular orbitals, one can see the optimum position as resulting from a trade-off between the repulsion of the positively charged nuclei and the attraction between each nucleus and the orbiting electrons. Energetically, the most favorable position of the electrons is between the nuclei, which leads to a mutual attraction between the O and H atoms. These competing effects tend to confine the two atoms to an optimum distance at the lowest point of a potential “well.” Any movement changing the length of the bond will be opposed by a counteracting force, which leaves the system in a perpetual state of vibration. We can represent such a system with two balls

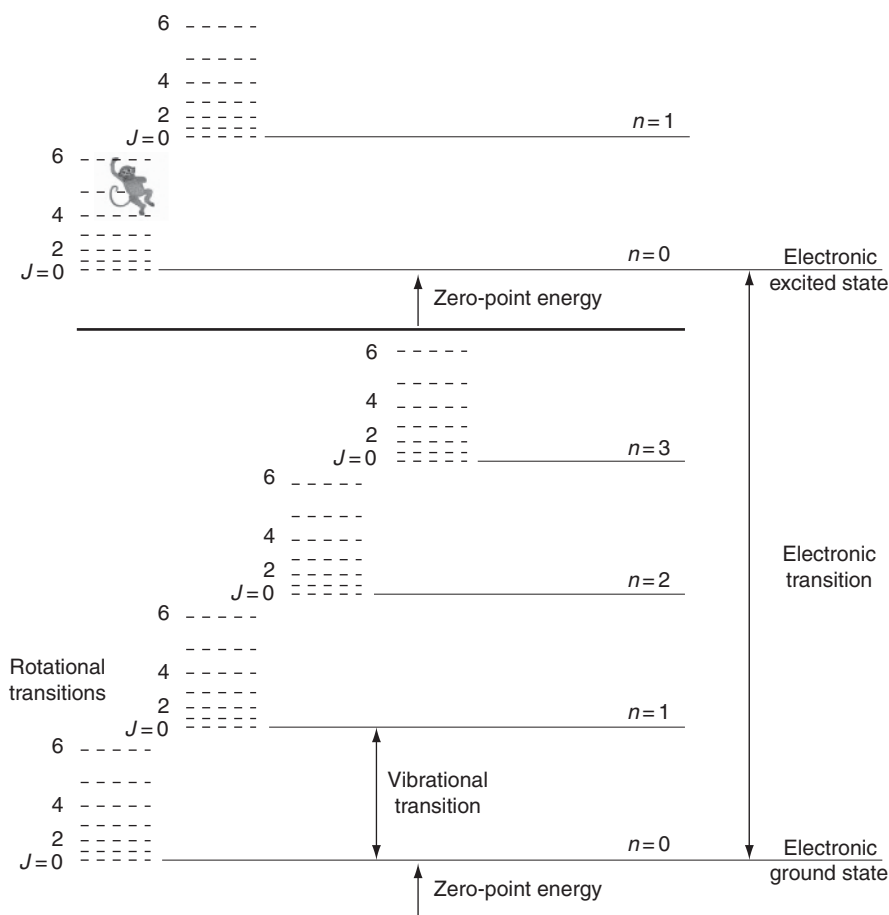


Figure 3.1

The different energy levels of a compound. The separation of the rotational energy levels (J is the number of rotational quanta) is very small with respect to the separation of the vibrational levels and that of electronic levels between different orbitals. Note the zero-point energy, a consequence of the uncertainty principle, which only appears for the vibrational energy levels.

attached by a spring: this is the model of the harmonic oscillator. College physics tells us that if such a system does not lose energy by friction or radiation, the sum of the potential and kinetic energies remains constant. The potential energy $V(r)$ of a diatomic molecule is a function of the separation distance r between the nuclei and goes through a minimum for $r = r_0$. The potential energy $V(r)$ can be expanded about the value at the minimum as

$$V(r) = V(r_0) + \left(\frac{dV}{dr} \right)_{r_0} (r - r_0) + \frac{1}{2} \left(\frac{d^2V}{dr^2} \right)_{r_0} (r - r_0)^2 + \dots \quad (3.3)$$

which assumes that terms with degrees > 2 , known as anharmonic, are small enough to be neglected: this is the parabolic or harmonic approximation of the potential well. The first term on the right-hand side is the energy at the minimum and the second is zero because the derivative is evaluated at the minimum. Let us call k the second-order derivative calculated

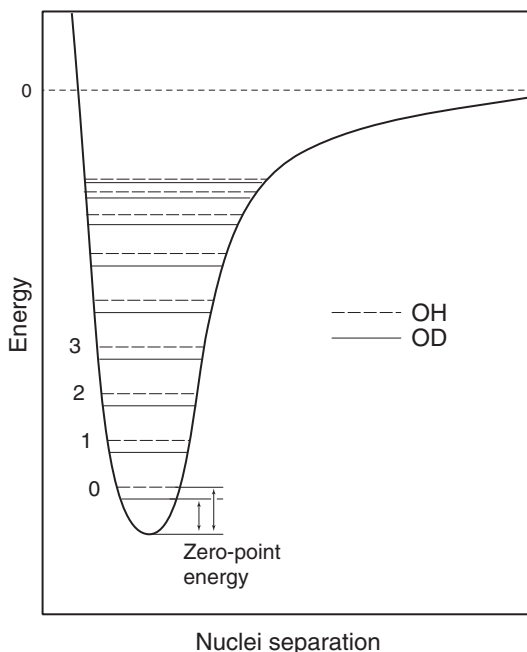


Figure 3.2 Energy of the oxygen—hydrogen bond. The potential of the O—H bond as a function of the distance between the two nuclei is shown as a continuous curve. The zero represents the energy of the system when O and H are fully dissociated. Because the heavy nucleus hardly budes when the light electrons wiggle, this curve is independent of the mass of the nuclei (Born–Oppenheimer approximation) and is therefore the same for all isotopes. The quantized energy levels ($n = 0, 1, 2, \dots$) are shown for the O—H (oxygen—hydrogen) and O—D (oxygen–deuterium) bonds. The first energy levels are nearly equally spaced. The isotopically heavier molecules are in a lower state of energy than the lighter molecules. Zero-point energy is the elevation of the ground state ($n = 0$) above the minimum of the potential well. Differences in zero-point energies between molecules with different isotopes (e.g. O—H and O—D) account for all stable isotope fractionation effects.

at r_0 and show that it measures the force of the spring. Stretching the bond by applying a force F increases its potential energy and this takes the form:

$$F = -\frac{dV}{dr} \quad (3.4)$$

with the minus sign ensuring that energy increases when the force stretches the bond. Comparing the two equations leads to Hooke’s law, which we already met in the previous chapter:

$$F = -k(r - r_0) \quad (3.5)$$

The constant k is therefore a measure of the “hardness” of the spring, i.e. of how much energy is needed to achieve a particular change in the bond length. Now, let us summon our college physics and remember one of Newton’s great discoveries: $F = M d^2r/dt^2$, where M is the mass, or force and acceleration are proportional.

Bringing everything together, we get:

$$\frac{d^2 (r - r_0)}{dt^2} + \frac{k}{M} (r - r_0) = 0 \quad (3.6)$$

in which we use the property that the derivative of r_0 is zero. Periodic functions of the form $\sin \sqrt{k/M}t$ clearly satisfy this equation. The most important parameter of this solution is the frequency of the oscillation $\nu = (1/2\pi) \sqrt{k/\mu}$. The harmonic mean mass (known as the reduced mass) μ such as $1/\mu = (1/M_O) + (1/M_H)$ arises because each atom actually carries out only part of the work it would have to do if it was attached to a steady support. As expected, heavy atoms do not jump around very quickly!

Upon formulation of black-body radiation theory, Planck laid the groundwork of quantum mechanics by hypothesizing that a system undergoing a periodic movement with frequency ν can only occupy the discrete energy states $E_n = nh\nu$, in which h is the Planck constant equal to 6.63×10^{-34} J s and $n = 0, 1, 2, \dots$. From observations on the photoelectric effect, Einstein postulated that the energy of an electromagnetic wave is actually bundled with the properties of a particle, the photon. Photons have no mass and no electric charge. Upon emission or absorption of photons, material shifts from one energy level to another, but the energy carried by each photon is always $h\nu$.

For the harmonic oscillator, the situation is slightly more complicated by the existence of the zero-point energy, without which, however, no fractionation of stable isotopes would exist. The relationship between the energy of our ball-and-spring system and frequency is:

$$E_n = \left(n + \frac{1}{2} \right) h\nu \quad (3.7)$$

with $n = 0, 1, 2, \dots$. Again, moving up and down the energy levels involves the absorption or the emission of photons with energy $h\nu$. This does not happen, however, for homonuclear, symmetrical diatomic molecules, such as H_2 and O_2 , which cannot change their vibrational and rotational energy level and explains why these gases are transparent (see [Sections 9.1](#) and [12.9](#)). The existence of zero-point energy E_0 for $n = 0$ is a result of the Heisenberg uncertainty principle: if the energy of the system was allowed to reach, as it is in classical physics, its minimum value, both the position ($r = r_0$) and the velocity ($\sqrt{2(E_0 - V_0)/m}$) of each atom would be precisely known, which is not permitted by the uncertainty principle. Such a limitation does not arise for rotational energy because the position of the atom on its orbit remains undetermined at all times. Vibrational zero-point energy is important for natural systems because at nearly up to ambient temperature, most oscillators are precisely at that energy level.

Not all the natural systems are simple diatomic harmonic oscillators. More complex molecules have more complex patterns of vibration. Fortunately, group theory allows us to make the situation more tractable and demonstrates that any arbitrary vibration of a molecule can be broken down into the superposition of simple “normal modes.” Most molecules made of N atoms have $3N - 6$ normal modes of vibration, whereas this number reduces to $3N - 5$ for linear molecules. [Figure 3.3a](#) shows some of the normal modes for some of the common gaseous species, OH, H_2O , CO_2 , CH_4 . The frequencies shown are well known to spectroscopists (infrared, Raman, ultraviolet) and are used to identify

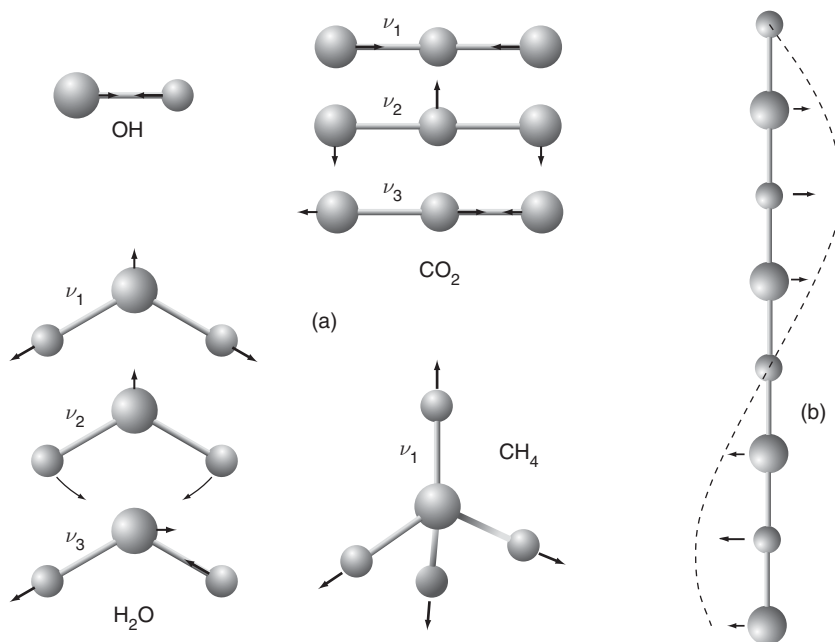


Figure 3.3

(a) Vibrations of molecules, OH, H₂O, CO₂, CH₄. All the vibrations, however complex, can be described as the superposition of a small number of normal modes (shown here as arrows) corresponding to different frequencies ν_1, ν_2, \dots measurable by infrared or Raman spectroscopy. (b) For solids, the vibrations take the form of traveling waves.

the presence of these gases in the molecular clouds of distant galaxies as well as in the terrestrial atmosphere.

Crystalline solids behave in yet another way (Fig 3.3b): because ions are regularly distributed and interact with their neighbors in a continuous way, vibrations take the form of traveling waves. The pseudo-particles associated with these waves are known as phonons. Models related to the statistical theory of the heat capacity C_V of solids – the increment of energy associated with a small temperature step – assume either a single vibration frequency (Einstein solid) or a frequency continuum increasing up to a cut-off value imposed by the lattice (Debye elastic solid). The Einstein and Debye models are reasonably successful for simple crystals, but the wealth of spectroscopic data and the advent of large computers have now made it possible to evaluate exact isotopic properties using so-called “ab initio” models. Models of fractionation involving liquid phases require particularly intensive numerical computing.

Where are the isotope effects in all this? Heavy atoms react more slowly than light ones and therefore tend to occupy lower energy levels. Bond energy varies with ν and therefore with $1/\sqrt{\mu}$, where μ is the harmonic mean mass of the atoms that form the molecule. A consequence of this rule is that the quantized energy levels and the zero-point frequencies are lower for a bond involving the heavier isotopes: the molecule OD is more stable than OH (Fig. 3.1). This can be seen for the substitution of H by D in magnesium hydroxide Mg(OH)₂ (brucite), which drastically reduces the frequency of the OH vibration (Fig. 3.4).

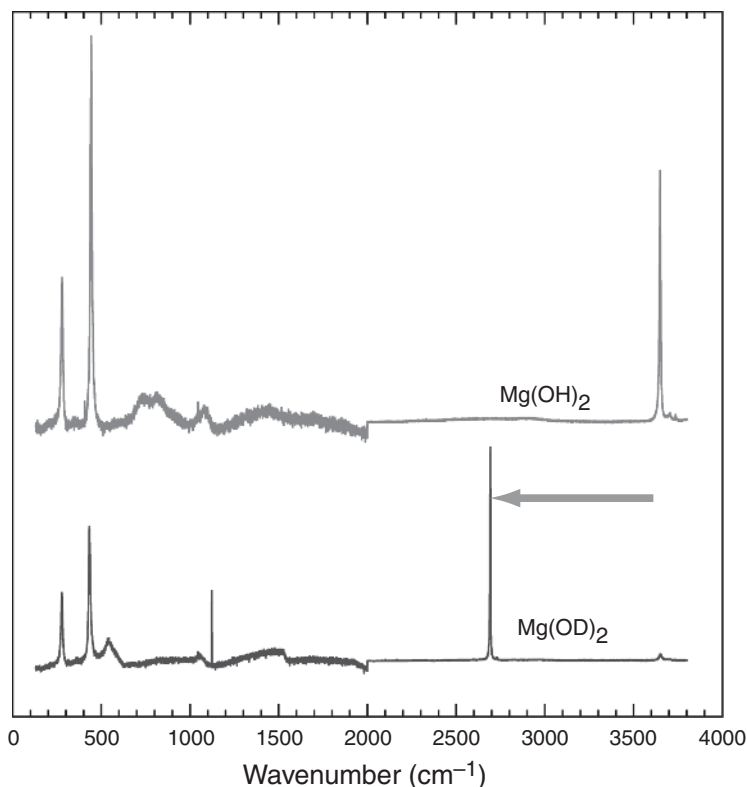


Figure 3.4

Energy shift in brucite ($\text{Mg}(\text{OH})_2$) induced by the substitution of D for H in the OH radical (courtesy of Bruno Reynard). Spectroscopists do not normally work with frequency but with wavenumbers, in cm^{-1} , which are frequencies divided by the velocity of light.

Let us go back to the exchange of ^{16}O and ^{18}O between water vapor and liquid water (3.1) and consider a vibrational mode with different hardness parameters $k_{\text{vap}} \ll k_{\text{liq}}$ indicative of loose bonds in the gaseous state (Fig. 3.5). The variation ΔE of energy during this exchange is

$$\Delta E = (E_{\text{H}_2^{18}\text{O}_{\text{vap}}} + E_{\text{H}_2^{16}\text{O}_{\text{liq}}}) - (E_{\text{H}_2^{18}\text{O}_{\text{liq}}} + E_{\text{H}_2^{16}\text{O}_{\text{vap}}}) \quad (3.8)$$

or

$$\Delta E = (E_{\text{H}_2^{18}\text{O}_{\text{vap}}} - E_{\text{H}_2^{16}\text{O}_{\text{vap}}}) - (E_{\text{H}_2^{18}\text{O}_{\text{liq}}} - E_{\text{H}_2^{16}\text{O}_{\text{liq}}}) \quad (3.9)$$

For the sake of illustration, let us assume that most of the atoms will occupy their ground, zero-point energy level ($n = 0$) so that:

$$\Delta E = \frac{1}{2}h \left[(\nu_{\text{H}_2^{18}\text{O}_{\text{vap}}} - \nu_{\text{H}_2^{16}\text{O}_{\text{vap}}}) - (\nu_{\text{H}_2^{18}\text{O}_{\text{liq}}} - \nu_{\text{H}_2^{16}\text{O}_{\text{liq}}}) \right] \quad (3.10)$$

$$= \frac{h}{4\pi} \left[(\sqrt{k_{\text{vap}}} - \sqrt{k_{\text{liq}}}) \left(\frac{1}{\sqrt{M_{\text{H}_2^{18}\text{O}}}} - \frac{1}{\sqrt{M_{\text{H}_2^{16}\text{O}}}} \right) \right] \quad (3.11)$$

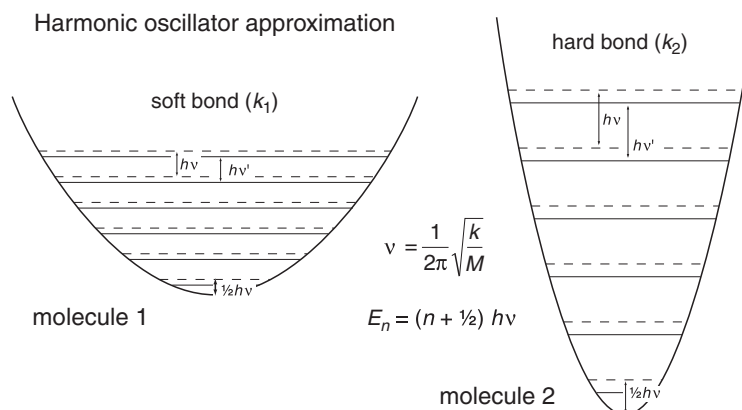


Figure 3.5

Comparison between two bonds, one soft (left) and one hard (right) with the force constant of the soft bond (k_1) less than that of the hard bond (k_2). The total energy is at a minimum when heavy isotopes preferentially populate the hard bond.

This quantity is clearly > 0 which indicates that, in order to achieve energy reduction, reaction (3.1) must proceed from right to left (backward). The heavy ^{18}O therefore fractionates preferentially into the liquid phase. It is a general result that heavy isotopes fractionate in favor of the stiffest bonds. Since transforming solid or liquid into vapor requires addition of energy to break bonds (latent heat), solids and liquids, where most of the energy is stored in vibrations, lower the total energy of the system by concentrating heavier isotopes. In contrast, vapor offers sites that are higher on the energy scale than the corresponding liquid and therefore tend to concentrate the lighter isotopes relative to the liquid. In a liquid–vapor equilibrium, such as H_2O liquid and vapor below 220°C , the liquid is enriched in the heavier isotope (e.g. ^{18}O , ^2H), while the vapor preferentially concentrates the lighter isotope (e.g. ^{16}O , ^1H).

The Boltzmann distribution

Let us consider N identical particles, atoms or molecules, which can occupy a large number of energy levels, n_1 being at the level E_1 , n_2 at the level E_2 , etc. We assume that each individual particle has an equal probability to land on any energy level. Without loss of generality, we will assume that N is the Avogadro number (1 mole). We are going to justify to some extent that the fractional proportions $f_i = n_i/N$ of these atoms or molecules that have the energy E_i at temperature T is:

$$f_i = \text{const} \times e^{-\frac{E_i}{RT}} \quad (3.12)$$

Our assumptions are that the occupancy of a particular energy level, say E_i , is independent of the occupancy of another level, say E_j . The function f therefore requires that $f_{i+j} = f_i \times f_j$. The only function with such a property is the exponential function, which suggests the form:

$$f_i = \text{const} \times e^{-\beta E_i} \quad (3.13)$$

The positive constant β is to be determined and the minus sign ensures that f_i remains finite. From the condition that the fraction proportions f_i sum to unity, we get the constant equal to Q^{-1} , where $Q = \sum_{i=0}^{\infty} e^{-\beta E_i}$ is known as the partition function. This can be recast as:

$$f_i = \frac{e^{-\beta E_i}}{Q} \quad (3.14)$$

In order to demonstrate that β is actually equal to $1/RT$, we need to pay a quick visit to the concept of entropy. Boltzmann formulated a statistical definition of the entropy S of a system as $R \ln \Omega$, where Ω is the number of indistinguishable microscopic configurations (how atoms distribute themselves among the possible states). The second principle then states that the entropy of an isolated system increases when it spontaneously evolves towards the state with the largest number of accessible configurations. The number Ω can be found using a simple argument: the total number of permutations of N atoms is $N!$, where the exclamation mark stands for the function factorial (e.g. $3! = 3 \times 2 \times 1$). Among the $N!$ permutations, $n_1!$ correspond to indistinguishable occupations of energy level E_1 with a similar outcome for other energy levels. The number of distinguishable configurations is therefore:

$$\Omega = \frac{N!}{n_1! n_2! \dots} \quad (3.15)$$

This expression would be a nightmare if it was not for the handy Stirling approximation $\ln N! \approx N \ln N - N$, valid for large N , and which gives a new expression for the entropy (remember that the logarithm of a product of numbers is the sum of the logarithms of these numbers):

$$\frac{S}{R} = +N \ln N - n_1 \ln n_1 - n_2 \ln n_2 - \dots - N + n_1 + n_2 + \dots \quad (3.16)$$

We now recall that $N = \sum_i n_i$; the second part of the right-hand side therefore vanishes and we get:

$$S = -R \sum_i f_i \ln f_i \quad (3.17)$$

Taking the differential of the entropy S at constant T :

$$dS = -R \sum_i df_i \ln f_i - R \sum_i \cancel{f_i} \frac{df_i}{f_i} \quad (3.18)$$

or, using (3.14)

$$TdS = RT\beta \sum_i E_i df_i - RT \ln Q \sum_i \cancel{df_i} \quad (3.19)$$

At constant volume, $\sum_i E_i df_i = dU = TdS$, which requires that $RT\beta = 1$. This ends the demonstration of one of the most important equations in science.

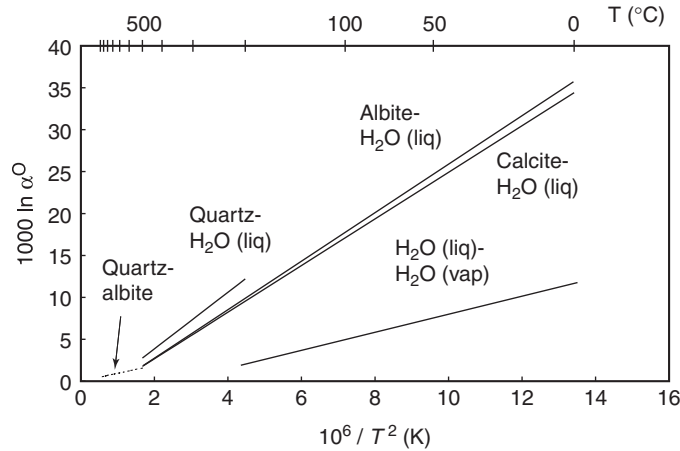


Figure 3.6 Fractionation of oxygen isotopes between a mineral phase and water, or between different mineral phases. Notice that preferential incorporation of ^{18}O is normally favored by the mineral structure and that isotopic fractionation decreases rapidly with increasing temperature.

Temperature may be understood through the Boltzmann distribution (see box), which determines the fraction of a population of atoms that populates a certain energy level. At moderately low temperatures, typically below ambient temperature, there is not enough energy to open up many vibrational levels and all the atoms are in their ground state. The exchange energy is constant and fractionation temperature dependent. In this case, which only finds useful applications when hydroxyl groups are involved, the law of mass action requires the temperature dependence of $\ln \alpha$ in $1/T$. Temperature in this case only attests to the total available vibrational energy and therefore indirectly constrains the relative occupation of the available levels. Higher temperatures have an additional effect: they open up new grounds for occupation. The more energy available, the more vibrational quanta can wander up the energy levels. In this case, which is a straight outcome of the quantum theory, we observe (Fig. 3.6) fractionation laws of the type:

$$\ln \alpha = \frac{A}{T^2} + C \quad (3.20)$$

where A and C are constants. These laws, to whom the names of Bigeleisen, Mayer, and Urey are attached for their 1947 papers, are widely used for thermometry of magmatic, metamorphic, or hydrothermal systems. The symmetry constant C is usually zero for isotopic exchange between anhydrous isotopomers so that fractionation at magmatic temperatures is normally small or negligible.

Since bond energy varies with the inverse square-root of the mean mass of the atoms that form the molecule (Eq. 3.11), the thermodynamic fractionation factor between isotopes generally falls very quickly with increasing mean atomic mass as it varies with the difference between smaller and smaller quantities. At 500–800 °C, fractionations of 20–80 per mil (‰) are commonly observed for the D/H ratio, of 2–8‰ for oxygen isotopes, and fall to less than 1‰ for zinc and copper isotopes.

A last effect deserves attention when we deal with molecules with very different degrees of symmetry. For example, the molecule CO has only one single possible configuration,

whereas the methane molecule can be reproduced identically to itself by rotating the CH₄ tetrahedron of $2\pi/3$ around any C–H bond: $4 \times 3 = 12$ indistinguishable configurations are therefore accessible to the same molecule. Methane thus has access to 12 times as many rotational states with respect to CO and, everything else being equal, its relative stability will be greatly enhanced with respect to that of carbon monoxide.

3.2 Delta notation and stuff

Using raw isotopic ratios to describe natural variability is very inconvenient because of their small amplitude. Also there is a common difficulty with interlaboratory biases. The same sample processed and analyzed by different groups on different instruments will come out differently and even sometime more differently than the actual natural variability. This is not a real issue because the knowledge of “true” isotopic ratios is practically pointless. Reproducibility is the magic word, not accuracy. The practice for all laboratories is to measure the same reference material so that each and every analyst can report his or her own data on unknown samples with respect to the same standard. Reference samples must be multiple, broadly available, homogenous, and they should be analyzed using the same analytical procedure as the unknown samples. Under these conditions, we expect that deviations of the isotopic composition from that of the reference, usually small numbers, should be known with great precision, typically 0.02 to 1‰ depending on the element and sample size.

The delta notation with respect to a particular reference material is generally used for isotopic ratios of stable nuclides; $\delta^{18}\text{O}$ and $\delta^{17}\text{O}$ represent the deviations of the isotopic $^{18}\text{O}/^{16}\text{O}$ and $^{17}\text{O}/^{16}\text{O}$ ratios in the sample in parts per thousand relative to the same ratio in the reference material. $\delta^{18}\text{O}$ is defined as:

$$\delta^{18}\text{O} = \left[\frac{(^{18}\text{O}/^{16}\text{O})_{\text{sample}}}{(^{18}\text{O}/^{16}\text{O})_{\text{ref}}} - 1 \right] \times 1000 \quad (3.21)$$

with the reciprocal expression of the isotopic ratio of a sample as a function of its $\delta^{18}\text{O}$ value:

$$\left(\frac{^{18}\text{O}}{^{16}\text{O}} \right)_{\text{sample}} = \left(\frac{^{18}\text{O}}{^{16}\text{O}} \right)_{\text{ref}} \left(1 + \frac{\delta^{18}\text{O}}{1000} \right) \quad (3.22)$$

It is common practice to use a light but abundant isotope in the denominator. Jargon refers to heavy oxygen for high $^{18}\text{O}/^{16}\text{O}$ ratios and to light oxygen otherwise.

A useful approximation of the fractionation properties is to compare the difference of $\delta^{18}\text{O}$ values between two co-existing phases 1 and 2 with the fractionation coefficients α of the same phases. The following notation is used:

$$\delta^{18}\text{O}_2 - \delta^{18}\text{O}_1 = 1000 \frac{(^{18}\text{O}/^{16}\text{O})_2 - (^{18}\text{O}/^{16}\text{O})_1}{(^{18}\text{O}/^{16}\text{O})_{\text{ref}}} \quad (3.23)$$

Since α is very close to one, we can use the approximation $\ln \alpha \approx \alpha - 1$ and insert it in the previous equation rewritten as:

$$\delta^{18}\text{O}_2 - \delta^{18}\text{O}_1 = 1000 \frac{\left(\frac{18\text{O}}{16\text{O}}\right)_1}{\left(\frac{18\text{O}}{16\text{O}}\right)_{\text{ref}}} (\alpha - 1) \approx 1000 \ln \alpha \quad (3.24)$$

in which we have taken into account that the ratio of two $^{18}\text{O}/^{16}\text{O}$ ratios is always very close to one. The difference in delta values between co-existing phases (minerals, liquids) therefore decreases as $1/T^2$, which implies that the sensitivity of stable-isotope thermometers decreases with increasing T , hence their important applications to low- and medium-temperature processes.

For elements with more than two isotopes, at constant temperature, the amplitude of fractionation α increases with the difference in mass of the isotopic ratios. For example, the difference in the $^{18}\text{O}/^{16}\text{O}$ ratio between two samples is twice the difference in the $^{17}\text{O}/^{16}\text{O}$ ratio. This is because bond energy varies with the mass of the bonding atoms. Therefore $\ln \alpha$ can be expanded to the first order relative to the difference in mass Δm in the isotope ratio, giving:

$$\ln \alpha (\Delta m) = \ln \alpha (\Delta m = 0) + f \Delta m + \mathcal{O}(\Delta^2 m) \quad (3.25)$$

where f , which is the derivative of $\ln \alpha$ relative to Δm for $\Delta m = 0$, is a coefficient that is independent of mass, termed mass discrimination. In this equation, \mathcal{O} means “of the order of” and we will neglect terms of higher than first order. Moreover, when the mass difference is zero, there is no fractionation between a mass and itself ($\alpha = 1$), and the first term on the right-hand side is therefore zero, giving for fractionation of ^{18}O and ^{16}O between phases 1 and 2 ($\Delta m = 2$):

$$\alpha_{2/1}^{\text{O}} = \left(\frac{18\text{O}}{16\text{O}}\right)_2 / \left(\frac{18\text{O}}{16\text{O}}\right)_1 = e^{2f} \quad (3.26)$$

When fractionation is small, i.e. when f tends toward 0, we utilize the linear approximation obtained by developing the logarithm of the left-hand side of (3.25) to the first order:

$$\alpha_{2/1}^{\text{O}} \approx 1 + 2f \quad (3.27)$$

We will have, for example, the two linear equations:

$$\left(\frac{17\text{O}}{16\text{O}}\right)_2 = \left(\frac{17\text{O}}{16\text{O}}\right)_1 (1 + f) \quad (3.28)$$

$$\left(\frac{18\text{O}}{16\text{O}}\right)_2 = \left(\frac{18\text{O}}{16\text{O}}\right)_1 (1 + 2f) \quad (3.29)$$

Alternatively, (3.27) can be re-written as

$$\frac{1 + \delta^{18}\text{O}_2/1000}{1 + \delta^{18}\text{O}_1/1000} \approx 1 + 2f \quad (3.30)$$

We use the approximation $(1 + x)^{-1} \approx 1 - x$ valid for small x and neglect the products of deltas to obtain:

$$\delta^{18}\text{O}_2 - \delta^{18}\text{O}_1 \approx 2000f \quad (3.31)$$

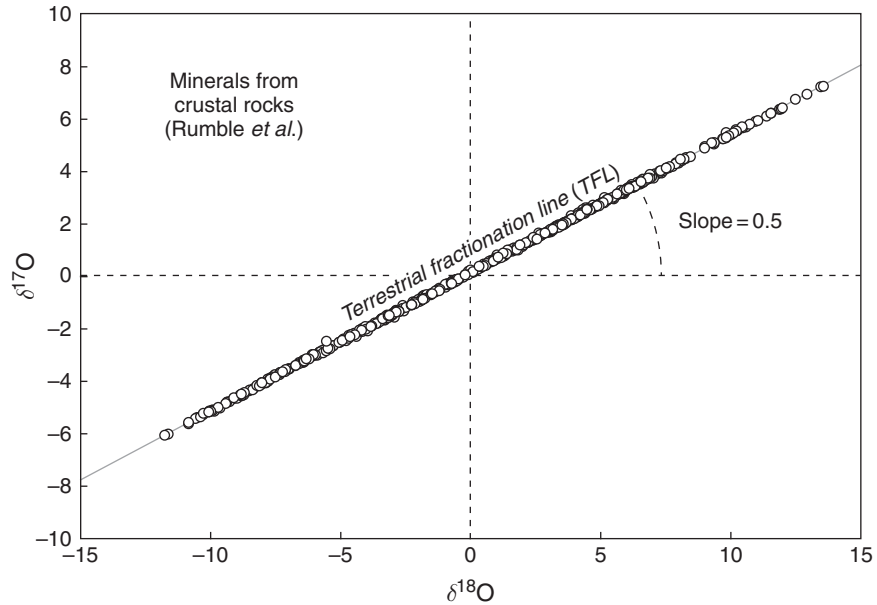


Figure 3.7

Relationship between $\delta^{17}\text{O}$ and $\delta^{18}\text{O}$ for >500 minerals from crustal rocks, mostly from China (Rumble *et al.*, 2007). The values define a nearly perfect straight line (errors are smaller than symbol size) going through (0,0) and with a slope of 0.5 demonstrating the perfect dependence of oxygen isotope fractionation on the mass difference between masses at the numerator and denominator. Laser ablation data by courtesy of Doug Rumble. Meteoric waters and sediments fall on the same line, called the terrestrial fractionation line.

Likewise for $\delta^{17}\text{O}$:

$$\delta^{17}\text{O}_2 - \delta^{17}\text{O}_1 \approx 1000f \quad (3.32)$$

In a plot with $x = \delta^{17}\text{O}$ and $y = \delta^{18}\text{O}$, isotope fractionation makes the isotope composition of sample 2 move on a straight line going through sample 1 with a slope of $\approx 1/2$ (see below for details on this value). This pattern is actually quite general and, for a planet starting with an isotopically homogeneous reservoir of oxygen, all the differentiation and mixing processes produce samples with $\delta^{17}\text{O}$ and $\delta^{18}\text{O}$ plotting on this very same straight line (Fig. 3.7). As we have not really assumed that fractionation takes place at equilibrium (we just used an expansion of $\ln \alpha$ with respect to Δm), kinetic and biological processes must also follow the same pattern. The $\delta^{17}\text{O}$ and $\delta^{18}\text{O}$ values of essentially all terrestrial samples plot on the terrestrial fractionation line (Fig. 3.7). It will be seen later that one very important application of this simple theory is in the discrimination of planetary material. The same principle holds for the isotopic variability of all the elements with more than two stable isotopes, such as Fe, Zn, and Mo: if Δm_x and Δm_y are the mass differences relative to the isotopic ratios used for x and y , respectively, the mass fractionation line has a slope of $\Delta m_y/\Delta m_x$. Some rare outliers exist, due to photodissociation reactions (different isotopes of the same element absorb radiations with slightly different wavelengths) or autocatalytic effects. Atmospheric sulfur with isotope ratios $^{34}\text{S}/^{32}\text{S}$ and $^{33}\text{S}/^{32}\text{S}$ and ozone are prime examples: these exotic processes are known by the name of mass-independent

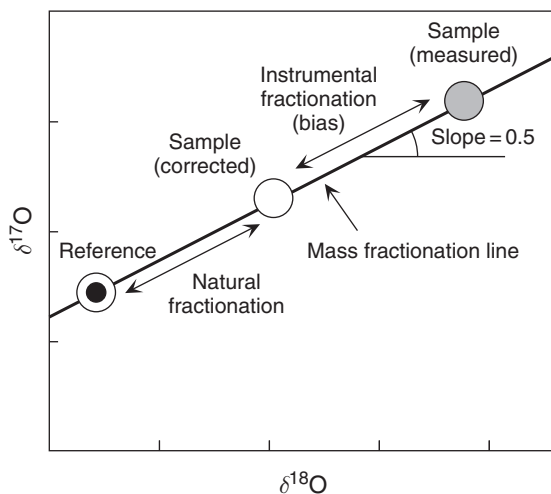


Figure 3.8 Fractionation depending on the mass of isotopes ^{16}O , ^{17}O , and ^{18}O is consistent whether its cause is natural or analytical. The $^{17}\text{O}/^{16}\text{O}$ and $^{18}\text{O}/^{16}\text{O}$ ratios are shown in delta notation. All samples from Earth lie on the same straight line of mass fractionation whose slope is equal to the ratio of the mass difference ($17 - 16$) by difference ($18 - 16$), i.e. 0.5. Natural fractionation is a deviation determined relative to an arbitrary reference sample, hence the δ notation. The isotopic bias is introduced by the mass spectrometric analysis and follows a similar mass-dependence law: it must be corrected for each sample by appropriate techniques.

fractionation. It is important to emphasize at this early stage that isotope measurements made in the laboratory report isotopic fractionation values that are the sum of fractionation related to the action of all natural processes *and* of instrumental fractionation, sometimes referred to as instrumental mass bias (Fig. 3.8). The true instrumental bias will never be known, except by artificially mixing pure isotopes into certified standard materials, but since every laboratory places – by definition – reference material at the same point in the diagram, this is something we can live with.

Let us finally note that, because we restricted ourselves to a first-order approximation, all the isotope fractionation laws seem to be giving a unique value for the slope of the fractionation line, e.g. 0.5 for oxygen. To higher orders, however, the data are good enough to tell one process from another, in particular whether isotope fractionation is controlled by quantum mechanics effects, with a dependence in $1/M$, or by kinetic effects, with a dependence in $\exp(-1/\sqrt{M})$, and to recognize the effects of Rayleigh distillation during phase change. This complex topic is beyond the scope of this textbook.

3.3 Hydrogen

It is important to remember that hydrogen is largely held in the hydrosphere, ocean, ice caps, and groundwater. The mantle may contain a large fraction of the terrestrial hydrogen inventory but its local concentrations are always small (a few hundred parts per million or

ppm). The consequence is that the hydrogen isotope compositions of aquifers are hardly modified by interaction with the ground, unless the proportion of groundwater held in the pores of the rock is extremely small.

On Earth, the average D/H ratio is about 1.4×10^{-4} , or equivalently, the isotopic abundance of D is 140 ppm. On Mars, the Viking landers measured a D abundance of 780 ppm. These numbers are much larger than the 20 ppm value of the solar nebula inferred from spectroscopic data on Jupiter and the reason is the faster escape rate of H from planetary atmospheres with respect to the twice-as-heavy D.

The reference material is the standard mean ocean water (SMOW), a man-made composite of various samples of desalinated seawater and δD usually refers to SMOW. Hydrogen isotopes fractionate very significantly between vapor and liquid and between vapor and ice under the temperature conditions prevailing at the surface of the Earth, which makes δD values universally employed tracers of the hydrological cycle. The factor 2 difference between the two isotopes is unique in the periodic table and accounts for the isotopic variability of δD that ranges up to several hundreds of per mil. Ice at the South Pole only contains 85 ppm D ($\delta D = -400$). At the temperatures of interest for environmental studies, vapor/liquid D/H fractionation varies from -170‰ at -25 °C to -110‰ at 0 °C , and -75‰ at $+25\text{ °C}$. As will be discussed in the next section, the isotope variability is amplified by the progressive distillation of rain and snow from the vapor transported by the atmosphere.

Fractionation of D from H is also observed between water and hydrous minerals. Although the experimental data are few and particularly difficult to interpret and to reproduce, hydrous minerals are typically depleted in deuterium by 30–50 per mil with respect to co-existing water and δD values of -40 may be found in minerals in equilibrium with seawater and in magmatic rocks altered by seawater. As expected, the effect of temperature is to reduce isotopic fractionation. The δD values of metamorphic and igneous hydrous minerals (chlorite, biotite, muscovite, amphibole) are typically in the range of -40 to -95‰ . Hydrogen isotope geochemistry therefore represents a powerful means of investigating the dehydration reactions associated with the burial of hydrous rocks, such as schists, serpentinites, and amphibolites, at subduction zones in particular, and the deep water cycle in general.

3.4 Oxygen

Oxygen has three stable isotopes at masses 16, 17, and 18, with average abundances of 99.76, 0.037, and 0.204 percent, respectively. For oxygen, as for hydrogen, the most broadly used reference material is the SMOW but low-temperature carbonate data are also commonly reported with respect to the carbonate of a belemnite from the Pee Dee formation (PDB), which is about 30 per mil heavier than SMOW. The $\delta^{18}\text{O}$ value of the Sun, as measured by the solar wind implanted in metal grains from the Moon regolith (Hashizume and Chaussidon, 2005) and by the cometary mission Stardust is about -40 to -60‰ . The mean terrestrial value is recorded by mantle rocks, which are the largest terrestrial reservoir

of oxygen, and is $\delta^{18}\text{O} \approx +5.5\%$. If atmospheric oxygen was in equilibrium with seawater, its $\delta^{18}\text{O}$ would be very similar to SMOW. Actually, its value is more like $\approx +23.5\%$. This is the Dole effect, which reflects the control of photosynthesis and respiration.

Fractionation of ^{16}O from ^{18}O between liquid water and vapor is about one order of magnitude smaller than for hydrogen isotopes, which is what is roughly expected from the comparison of $\sqrt{18/16} - 1$ and $\sqrt{2/1} - 1$. At the temperatures of interest for environmental studies, vapor/liquid $^{18}\text{O}/^{16}\text{O}$ fractionation is only mildly temperature dependent: -15% at -25°C , -12% at 0°C , and -9% at $+25^\circ\text{C}$. Because temperature is the only variable and is common to both systems, it is expected that δD and $\delta^{18}\text{O}$ should be strongly correlated in rain waters (and snow). The linear relation $\delta\text{D} = 8\delta^{18}\text{O} + 10$ discovered by Craig in 1961 and called the Global Meteoric Water Line (GMWL) can be explained by a process of fractional condensation of water vapor upon migration of moist equatorial air toward the poles. The SMOW does not plot on this line simply because water vapor is isotopically fractionated with respect to surface seawater. Let us write the Rayleigh equation for the number of moles n of each isotope left in the atmosphere with D^i being the partition coefficient of isotope i between water and vapor as:

$$d \ln n_{\text{vap}}^{18\text{O}} = \left(D_{\text{liq/vap}}^{18\text{O}} - 1 \right) d \ln f \quad (3.33)$$

$$d \ln n_{\text{vap}}^{16\text{O}} = \left(D_{\text{liq/vap}}^{16\text{O}} - 1 \right) d \ln f \quad (3.34)$$

in which f is the mass fraction of vapor left; and subtract the second equation from the first. We obtain:

$$d \ln \left(\frac{^{18}\text{O}}{^{16}\text{O}} \right)_{\text{vap}} = \left(D_{\text{liq/vap}}^{18\text{O}} - D_{\text{liq/vap}}^{16\text{O}} \right) d \ln f \quad (3.35)$$

$$= D_{\text{liq/vap}}^{16\text{O}} \left(\alpha_{\text{liq/vap}}^{18\text{O}/16\text{O}} - 1 \right) d \ln f \quad (3.36)$$

where we have simply introduced the original definition (3.2) of α . A similar expression holds for D/H. We now observe that, because ^{16}O and H are the dominant oxygen and hydrogen species in both the liquid and the vapor, $D_{\text{liq/vap}}^{16\text{O}}$ and $D_{\text{liq/vap}}^{\text{H}}$ are both very close to unity and introduce the approximation $d \ln \text{D}/\text{H} = d \ln (1 + \delta\text{D}/1000) \approx d\delta\text{D}/1000$. After this replacement has been made, we divide the same expression for D/H by the last equation, and we get the slope of the GMWL as:

$$\left(\frac{d\delta\text{D}}{d\delta^{18}\text{O}} \right)_{\text{vap}} \approx \frac{\alpha_{\text{liq/vap}}^{\text{D}/\text{H}} - 1}{\alpha_{\text{liq/vap}}^{18\text{O}/16\text{O}} - 1} \quad (3.37)$$

From the equation describing the isotopic evolution of the vapor, we now proceed to derive the $\delta\text{D}-\delta^{18}\text{O}$ relationship in precipitations. Equation (3.24) shows that rain and snow samples are just shifted from the vapor line towards more positive values by the factors $100 \ln \alpha_{\text{liq/vap}}^{\text{D}/\text{H}}$ for x and $1000 \ln \alpha_{\text{liq/vap}}^{18\text{O}/16\text{O}}$ for y but the slope of the precipitations is identical to that of the vapor. This fully justifies the correlation between δD and $\delta^{18}\text{O}$ observed by Craig.

Among the processes that fractionate oxygen isotopes at low temperature, probably the most important is between water and the different forms of dissolved and crystallized carbonates. This was understood in 1947 by Urey and his students who first identified the potential of this technique for paleothermometry. Kim and O'Neil (1997) made a very careful investigation of $^{18}\text{O}/^{16}\text{O}$ fractionation between calcite and water and suggested the expression:

$$1000 \ln \alpha_{\text{calcite/water}}^{^{18}\text{O}/^{16}\text{O}} = \frac{18030}{T} - 32.42 \quad (3.38)$$

Fractionation is prone to effects of salinity. The different carbonate ions H_2CO_3 , HCO_3^- , and CO_3^{2-} have very different $\delta^{18}\text{O}$ values, decreasing in that order. Today, the oxygen isotope geochemistry of foraminifera has become the essential tool for establishing temperature and salinity in the ancient oceans. Seawater $^{18}\text{O}/^{16}\text{O}$ changes only by addition of melt water, which is meteoric water with very different isotopic properties, and we will see that this is actually used to trace the evolution of the ice caps. If this effect can be neglected, the $\delta^{18}\text{O}$ of a marine calcite fossil may be used to infer the temperature of the seawater in which the animal grew. Fractionation of oxygen isotopes in phosphates (e.g. especially tooth enamel) are used in the same way.

Because of prominent temperature effects, oxygen isotope geochemistry provides unique constraints on the origin of igneous and metamorphic rocks:

1. Magmatic differentiation of basaltic rocks takes place at temperatures of about 1100°C and therefore does not entail any significant fractionation of oxygen isotopes (< 0.4 per mil) (Fig. 3.6). The $\delta^{18}\text{O}$ values of most fresh basaltic rocks derived from either glass or olivine fall in the range $5.2\text{--}5.8\text{‰}$ which is within 0.3 per mil of mantle values.
2. Partial melting at temperatures in excess of 800°C creates no or minimal isotope fractionation.
3. Large deviations of $\delta^{18}\text{O}$ values from the mantle values require that either some source rocks were once involved in low-temperature processes (they contain sediments or altered rocks) or that the samples was exposed to hydrothermal alteration or weathering.
4. The order of decreasing $\delta^{18}\text{O}$ at equilibrium should be quartz, feldspar, Fe–Mg silicates, magnetite. The commonest rocks in the continental crust derive largely from the metamorphic transformation of sediments (schist, gneiss) and their melting (granite).

Fig 3.6 also shows the $^{18}\text{O}/^{16}\text{O}$ fractionation between albite and water, which cuts across all the other curves. A first implication is that exchanged silicates at hydrothermal and surface temperatures have $\delta^{18}\text{O}$ values much higher than the co-existing water: clay minerals are enriched by about $12\text{--}25$ per mil with respect to seawater in the temperature range of $150\text{--}25^\circ\text{C}$. This shift is clearly visible in the high $\delta^{18}\text{O}$ values of altered oceanic basalts. It also explains the role that the sedimentary cycle plays with respect to the continental crust. The consistently high $\delta^{18}\text{O}$ values (typically $+7$ to $+15\text{‰}$) of gneiss and mica-schist, but also of the anatectic granites which form by melting of these metamorphic rocks reflects this so-called metasedimentary origin. Such high $\delta^{18}\text{O}$ values of silicic metamorphic and magmatic rocks with respect to the mantle value ($\approx +5.5\text{‰}$) require the

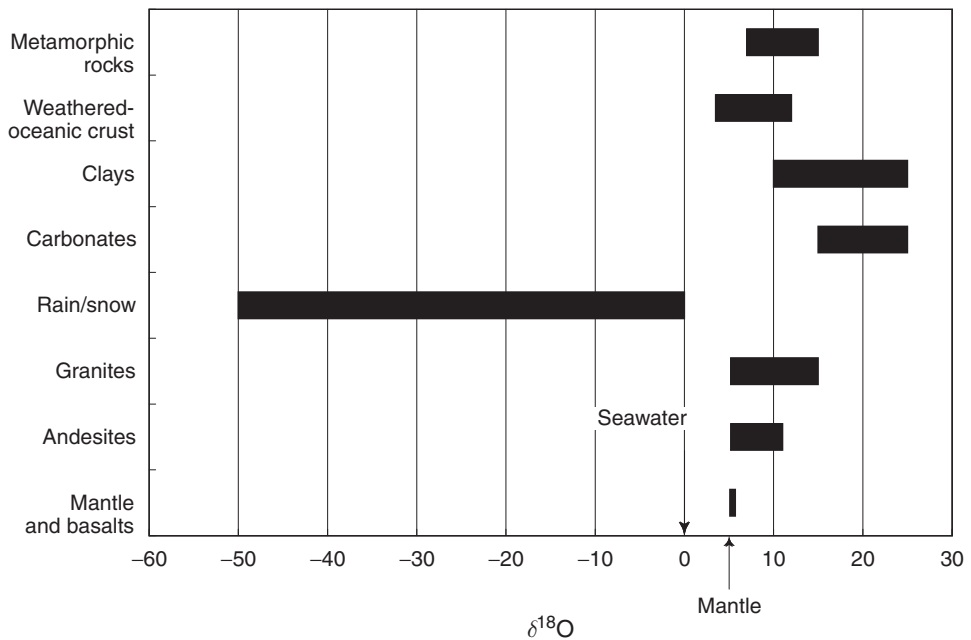


Figure 3.9

Distribution of $\delta^{18}\text{O}$ values in rocks and natural water. Notice seawater at 0‰ and the Earth's mantle at 5.5‰. It is the equilibration of sedimentary and metamorphic rocks with seawater at low temperature that raises the $\delta^{18}\text{O}$ of these rocks and lowers that of seawater. The broad isotopic variation of meteoric water results from atmospheric precipitation, which occurs at low temperature.

presence in their source material of rocks and minerals that have been subjected to low-temperature interaction with a hydrous fluid, such as seawater, groundwater, or meteoric water.

Conversely, upon interaction of rocks with seawater at temperatures of $\approx 300^\circ\text{C}$, the reversal of albite–water $^{18}\text{O}/^{16}\text{O}$ fractionation drags these rocks towards lower $\delta^{18}\text{O}$ values. This is also clearly visible in the low $\delta^{18}\text{O}$ values of the gabbroic section of ophiolites, widely regarded as the deep section of the oceanic crust exposed to circulating seawater at such temperatures.

The distribution of oxygen isotopes in the natural environment is summarized in Fig. 3.9. Marine alteration, especially the interaction of seawater with mid-ocean ridges, is thought to be responsible for the current $^{18}\text{O}/^{16}\text{O}$ ratio of seawater: throughout the Earth's history, seawater has circulated in submarine hydrothermal systems and its oxygen has been brought into isotopic equilibrium at average temperatures of the order of 275°C with the oxygen of basalts erupted by the volcanic systems of mid-ocean ridges. To these purely thermal effects must be added that of interaction with ^{18}O - and D-depleted meteoric water, which, as discussed below, is quite spectacular in modern and fossil peri-magmatic geothermal fields. Oxygen and hydrogen isotope evidence on shallow intrusions indicates that even the most fresh-looking plutonic rocks may have interacted with fluids contaminated by meteoric fluids.

3.5 Carbon

Carbon has two isotopes 12 and 13 with abundances of 98.89 and 1.11 percent, respectively. The universally accepted standard of $\delta^{13}\text{C}$ is the Pee Dee belemnite carbonate (PDB). Carbon is less abundant than oxygen but nevertheless ubiquitous. The major reservoirs are located in the mantle and in sedimentary carbonates. The different forms of carbonate ions dissolved in the ocean (H_2CO_3 , HCO_3^- , and CO_3^{2-}) and atmospheric CO_2 are minor reservoirs with respect to carbonates and mantle carbon but are particularly important to us. Carbon can be in reduced (C, CH_4 , organic material) or oxidized form (CO , CO_2). It is under different forms in the mantle and the relative abundances of these forms are not well constrained, but the “terrestrial” value of $\delta^{13}\text{C}$ should not be very different from -7‰ .

The core reaction of carbon isotope geochemistry is the following:



Contrary to all the substitutions we have seen so far, the two carbon molecules involved in this reaction have very different configurations and therefore very different normal modes of vibration (Fig. 3.3). In addition, the number of symmetrical configurations of the reactants and the products is very different. Isotope fractionation induced by such a reaction is therefore particularly strong, especially at low temperatures: the $\delta^{13}\text{C}$ of CO_2 is higher than that of CH_4 by 80 per mil at 0°C , 33 per mil at 200°C , and by 10 per mil at 700°C . This is a strong indication that biological processes must have a profound impact on the carbon isotope compositions of carbon-bearing systems. From left to right, the previous chemical reaction produces oxidative energy and is a mockup of respiration, which liberates CO_2 with high $\delta^{13}\text{C}$. Solar energy is needed to activate the non-spontaneous reaction from right to left: this is the essence of photosynthesis, which liberates oxygen and stores low- $\delta^{13}\text{C}$ reduced carbon in plants. Why is it that the final products do not have the same isotope compositions as the initial product such as suggested by the reaction? It is simply that the reactions are much more complicated and involve repeated exchanges of carbon inside the cell during which intermediate products are lost. For respiration, the excreted CO_2 is isotopically buffered by the biological material.

In addition to fractionation between reduced carbon and CO_2 , $^{12}\text{C}/^{13}\text{C}$ also fractionates at low temperature between atmospheric CO_2 , the dissolved carbonate species, and CaCO_3 carbonates with $\delta^{13}\text{C}$ being typically 10 per mil higher at 15°C in calcite than in atmospheric carbon dioxide.

The fractionation just referred to concerns the distribution of isotopes between phases in equilibrium, but another type of fractionation (kinetic isotope effect or KIE) takes place when species with different oxidation states and coordination (here CO_2 and CH_4) fail to achieve equilibrium, in particular during biological reactions. For example, carbonic anhydrase enzyme found in mammal blood speeds up the conversion of CO_2 into an HCO_3^- ion by five orders of magnitude, thus preventing bubbles of excreted CO_2 from forming. Light isotopes having higher vibrational frequencies enter into reaction paths more often than heavy isotopes and are therefore exchanged more readily. They are also bound less

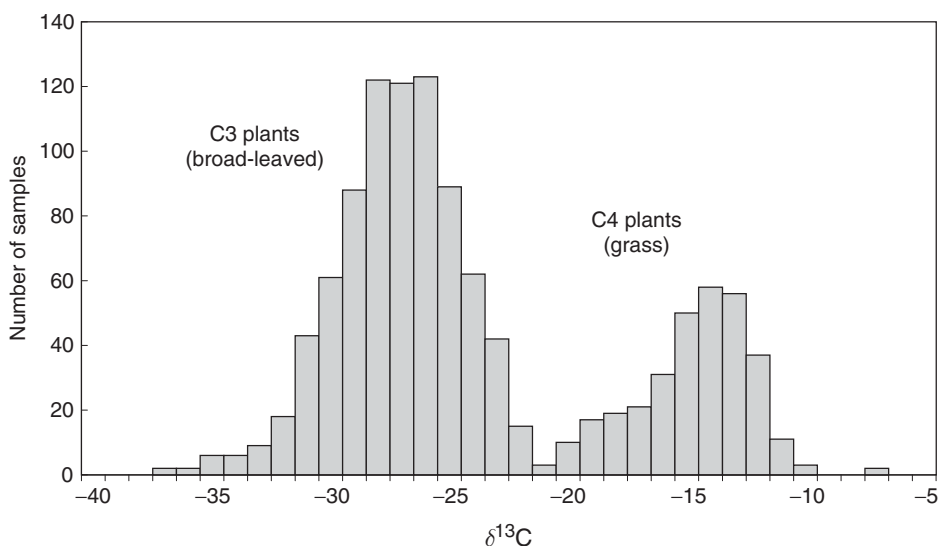


Figure 3.10 The effect of the metabolic cycle on the fractionation of carbon isotopes during photosynthesis. The C3 cycle (broad-leaved plants) and C4 cycle (grasses) correspond to very different photosynthetic processes within the cell. Past climatic conditions can therefore be inferred from the $\delta^{13}\text{C}$ value of organic remains (Deines, 1980).

strongly than heavy isotopes. In particular for fast reaction rates, equilibrium is therefore not necessarily achieved. Thus, by comparison with the environment within which they formed, organic products are significantly depleted in ^{13}C relative to ^{12}C . Such isotopic effects are extensively used in studying the genesis of fossil fuels and low-temperature mineralization in which biological processes are important, and in fingerprinting traces of early life in Archean sediments.

Since the isotopic standard of this element is the PDB marine carbonate, marine carbonates, as a whole, have $\delta^{13}\text{C}$ values close to 0‰. The carbon in atmospheric CO_2 has a $\delta^{13}\text{C}$ value close to -7 ‰. The continental biomass (dominated by plants), in contrast, has very negative $\delta^{13}\text{C}$ values. The distribution has two maxima, one at about -14 ‰, corresponding generally to grasses, and a larger one at about -25 ‰, corresponding to most broad-leaved plants (Fig. 3.10). This contrasted fractionation demonstrates that photosynthesis does not take place at equilibrium. It is brought about by two different CO_2 fixation mechanisms by very different plants, with what are known as the C4 pathway, predominating for grasses, and the C3 pathway, for broad-leaved plants and conifers. The very negative values of the C3 plants are essentially due to intracellular kinetic fractionation during C fixation mediated by the enzyme known as “rubisco.” The variation in $\delta^{13}\text{C}$ of fossil plant matter collected from bores in peat bogs is thus utilized for tracing changes in vegetation between glacial and interglacial periods. Increased $\delta^{13}\text{C}$ levels of organic matter are interpreted as marking the advance of grasslands, while very negative $\delta^{13}\text{C}$ levels indicate a return of broad-leaved plants. The $\delta^{13}\text{C}$ of ≈ -25 ‰ of bitumen is inherited from their vegetal precursors. Carbon in oil tends to be even lighter.

Phytoplankton, which dominates primary productivity at the surface of the oceans, has a $\delta^{13}\text{C}$ value of about -25‰ . Where organic-matter productivity is intense, there is a corresponding depletion of surface water in ^{12}C . The carbon of carbonates that form the tests of calcareous algae (such as, in particular, coccoliths that form chalk) and of foraminifera that graze on plankton (such as globigerina) reflects the intensity of this depletion. The $\delta^{13}\text{C}$ values of foraminifera in carbonate sediments serve as a measuring rod for the biological productivity of ancient oceans where the sedimentation occurred.

The $\delta^{13}\text{C}$ values of most diamonds (known as peridotitic), carbonatites (magmas essentially made of carbonates such as those produced by the Oldoinyo Lengai volcano, Tanzania) and volcanic gases cluster around -7‰ . This isotope composition is considered to be representative of deep-seated carbon. It is coincidentally very similar to atmospheric carbon. Undegassed mid-ocean ridge basalts also have similar values, but CO_2 outgassing drives the $\delta^{13}\text{C}$ of the residual carbon towards -20‰ .

3.6 Sulfur

Sulfur has four isotopes of masses 32, 33, 34, and 36 with mean abundances of 95.0, 0.75, 4.21, and 0.02 percent, respectively. Because of their small abundances, isotope 33 is rarely measured while isotope 36 is left out, so that the bulk of the geochemical information comes from the $^{34}\text{S}/^{32}\text{S}$ ratio only. Most of the S element inventory is confined to the mantle and the core, but sulfate is one of the major components of seawater while calcium sulfate and iron sulfide make up an important component of sediments. For decades, the accepted standard was the Canyon Diablo Troilite (CDT). Troilite (FeS) is a sulfide found as large blebs in the Canyon Diablo iron meteorite, which excavated Meteor Crater in Arizona. After evidence was found that CDT was not truly homogeneous, it has been replaced by a synthetic silver sulfide (Ag_2S) produced by the International Atomic Energy Agency. Because the surface reservoirs are presumably small with respect to the deep ones, the mean terrestrial $\delta^{34}\text{S}$ is probably very close to zero.

As for carbon, the most interesting aspects of sulfur stable isotopes are related to competing dominant states of oxidation, H_2S , SO_2 , and SO_3 in the gas phase, S^{2-} (sulfide), SO_3^{2-} (sulfite), and SO_4^{2-} (sulfate) in solutions and ionic compounds. As for carbon, isotopic equilibrium is rarely attained and kinetic isotope effects are important whenever redox and biological processes prevail. The trend is the same as with carbon: oxidized species are heavy (high $\delta^{34}\text{S}$ values), whereas the reduced species are light. It is easier to discuss fractionation in the gas phase; SO_2 is heavier than H_2S by 38 per mil at 0°C , 15 per mil at 200°C , and 4 per mil at 700°C . Under the same conditions, SO_3 , which hydrates into sulfate, is heavier than H_2S , which hydrates into different sulfide ions, by 80, 33, and 4 per mil, respectively. In general sulfide and sulfate in equilibrium at ambient temperature precipitate from solutions with a difference of about $+20$ in favor of the sulfate. Today's marine sulfate has a $\delta^{34}\text{S}$ of about $+20\text{‰}$, and so do modern marine evaporites: the very large isotopic difference with CDT demands the existence of a very large deep reservoir of 34-S depleted sulfur and therefore reflects the fact that the dominant mass of sulfur is in the

mantle. We can also expect that diagenetic reduction of marine sulfate, whether inorganic or biologically mediated, results in sulfides (often present in organic-matter-bearing sediments such as pyrite FeS_2) with $\delta^{34}\text{S}$ values a few tens of per mil below the marine value largely due to kinetic isotope effects. The $\delta^{34}\text{S}$ value of marine sulfate has fluctuated by several per mil over the Phanerozoic (see [Chapter 9](#)), which reflects changes in the burial of sedimentary pyrite and atmospheric oxygen pressure.

Sulfur isotopes have developed into a tracer of sulfide ore genesis thanks to the complex speciation of this element in solution. First, the diprotic acid H_2S dissociates into HS^- and S^{2-} as a function of pH and the dissociation constants vary with, among other parameters, temperature. Second, fractionation of sulfur isotopes between sulfate and sulfide species, either at equilibrium or kinetically controlled, is assumed. Depending on the pH and redox potential of the solution, different proportions of these species coexist and each of them has a different $\delta^{34}\text{S}$ value. Sulfides, such as pyrite, and sulfate, such as barite, can precipitate with a range of $\delta^{34}\text{S}$ that reflects these conditions. Using these principles, it can be demonstrated that the sulfur from black smokers is largely – although non exclusively – contributed by reduced basaltic sulfide and not by marine sulfate.

True igneous sulfides are rare because they are quickly oxidized by hydrothermal fluids. Nickel sulfide (pentlandite) is an all-too-rare truly magmatic sulfide in peridotites and basalts and its $\delta^{34}\text{S}$ is often close to zero.

Recently, the minor isotopes 33 and 36 of sulfur have found novel applications. First, photochemical reactions between solar ultraviolet radiations and SO_2 in the upper atmosphere create strong deviations from the mass-dependent fractionation relationships $\delta^{33}\text{S} = (1/2)\delta^{34}\text{S}$ and $\delta^{36}\text{S} = 2\delta^{34}\text{S}$. We will return to this point upon discussion of the rise of atmospheric oxygen. Second, because isotope fractionation between sulfides and sulfates is often large, the linear approximation of the Rayleigh law, which we met for O and H isotopes in meteoric waters, breaks down at the level of precision obtained by modern mass spectrometers. Small non-mass-dependent effects can thus be detected that seem to be powerful tracers of microbiological activity.

3.7 Nitrogen

Nitrogen has two isotopes 14 and 15, with mean abundances of 99.63 and 0.37 percent, respectively. The standard is, not surprisingly, atmospheric nitrogen (AIR). Although N_2 is the main component of the atmosphere, it has been argued that a substantial proportion is in the mantle. In addition, $^{15}\text{N}/^{14}\text{N}$ in extra-terrestrial material varies a lot as a result of loss from planetary atmospheres. We will therefore abstain from proposing a mean terrestrial value of $\delta^{15}\text{N}$.

As with carbon and sulfur, fractionation is dominated by nitrogen species of different oxidation states, N_2 , NH_3 , NO , NO_2 in the gaseous state and, for the last three, their dissolved equivalents, ammonium NH_4^+ , nitrite NO_2^- , and nitrate NO_3^- . At equilibrium under surface temperature conditions, nitrites and nitrates are isotopically heavier, and NH_3 is lighter than N_2 . Again, kinetic isotope effects are important. Biological processes play a

key role in defining the nitrogen isotope compositions of surface material. Fixation converts atmospheric nitrogen into ammonium needed for amino acids with variable depletions in ^{15}N , i.e. $\delta^{15}\text{N} = 0$ to -27% . Nitrification is an exothermic reaction that turns organic ammonium from mostly reduced amino (NH_2) groups into nitrite then nitrate. The yield of nitrification being close to 100 percent, the end products are variably depleted in ^{15}N . Reduction of marine nitrate into N_2 , called denitrification, is a very active process taking place in interstitial waters below the water–sediment interface: isotopically light N_2 is lost to the atmosphere, while the heavier residual nitrates are flushed back into the ocean. This explains the $\delta^{15}\text{N}$ of $\approx +5\%$ of deep-sea nitrates.

Nitrogen is surprisingly abundant in diamonds in which its $\delta^{15}\text{N}$ is $\approx -7\%$. There is a clear difference in nitrogen isotope compositions between mid-ocean ridge (-4) and ocean island basalts ($+3$), yet with significant overlap. The interpretation of these variations is still unclear but they seem to be related to how much recycled lithosphere is present in the source of each type of basalt.

3.8 Other elements

Recent progress in analytical techniques has opened up new grounds for stable isotope geochemistry. Besides boron, which we will see later can be used as a pH-meter of ancient oceans, and silicon, which is currently revived as a paleoceanographic tracer, the use of the isotope compositions of some metals has recently attracted considerable attention. Lithium has an interesting cycle giving information on fluid–rock interactions and subduction-zone processes. Magnesium and calcium are relevant to weathering and erosion cycles, molybdenum to redox conditions in the ocean and in diagenesis, Fe, Cu, Zn to biological processes and ore-body genesis, and selenium to environmental studies in changing redox conditions.

Exercises

1. Consider oxygen gas and the reaction $^{16}\text{O}_2 + ^{18}\text{O}_2 \rightleftharpoons 2^{16}\text{O}^{18}\text{O}$. What is the number of distinguishable configurations of each of the molecules involved in the reaction? If oxygen isotopes were distributing themselves at random in proportion to their abundances in the system and without any other effects, calculate the α value of this reaction.
2. The $\delta^{18}\text{O}$ value of modern seawater is 0% while the average value of the polar ice cap is -45% . The ice cap holds 2 wt% of the oceanic water. Calculate the $\delta^{18}\text{O}$ value of an ice-free ocean. Other water reservoirs can be neglected.
3. The $\delta^{18}\text{O}$ values of benthic carbonates (PDB scale) decreased from -1.2% to -2.5% between the Early Eocene and the Oligocene. Assume an ice-free ocean (no salinity variation) and determine the cooling of the deep ocean over the same period using

Table 3.1 Temperature coefficients of $1000 \ln \alpha_{\min}^{\text{O}} = A_{\min} T^{-2} + C_{\min}$ for different minerals. Third column: values of $\delta^{18}\text{O}$ in minerals from the same gneiss samples

Mineral	$10^{-6} A_{\min}$	C_{\min}	$\delta^{18}\text{O} \text{ ‰}$
Feldspar	3.38	-2.92	9.2
Plagioclase	2.76	-3.49	7.6
Magnetite	-1.47	-3.70	0.3
Muscovite	2.38	-3.89	6.6

Table 3.2 Coefficients of $1000 \ln \alpha_{\min}^{\text{O}} = AT^{-2} + BT^{-1} + C$ for the liquid water-vapor oxygen and hydrogen isotope exchange reactions

	$10^{-6} A$	$10^{-3} B$	C
α^{O}	1.137	-0.4156	-2.0667
α^{D}	24.844	-76.248	52.612

the equation $\delta^{18}\text{O}_{\text{calcite}} - \delta^{18}\text{O}_{\text{seawater}} = 2.78 \times 10^6 T^{-2} - 2.91$, where T is the absolute temperature.

4. Explain why δD and $\delta^{18}\text{O}$ in ice cores can be used to trace local precipitation temperatures.
5. Oxygen isotope thermometry of a metamorphic rock. The oxygen isotope compositions of minerals from a gneiss sample have been measured and reported in [Table 3.1](#). Let us call α_{\min}^{O} the value of the $^{18}\text{O}/^{16}\text{O}$ fractionation coefficients between minerals and water. The temperature dependence of this coefficient can be written as $1000 \ln \alpha_{\min}^{\text{O}} = A_{\min} T^{-2} + C_{\min}$ in which A_{\min} and C_{\min} are mineral-specific constants and T is the absolute temperature. The values of A and C are reported in [Table 3.1](#) for the different minerals. What is the quartz–magnetite apparent equilibration temperature? Plot $(\delta^{18}\text{O} - C)$ for each mineral vs. A : what is the slope of this alignment? What is the $\delta^{18}\text{O}$ value of the water in equilibrium with this mineral assemblage?
6. Explain why even subtle variations of $\delta^{18}\text{O}$ values in fresh basaltic glasses are said to indicate a source component processed at low temperature.
7. Let us call α^{O} the value for $^{18}\text{O}/^{16}\text{O}$ vapor/liquid fractionation in water and α^{D} the ratio for D/H fractionation. Using the values listed in [Table 3.2](#) calculate these coefficients at 5°C and 25°C . Calculate the $\delta^{18}\text{O}$ and the δD values of water vapor in equilibrium with seawater at 25°C . This water vapor now condenses as rain at 5°C . Using the Rayleigh fractionation law, calculate the $\delta^{18}\text{O}$ and the δD values of rain water when 10, 20, 50, and 80 wt% of the water vapor have condensed. Plot the corresponding δD vs. $\delta^{18}\text{O}$ values and compare the slope of the alignment with the meteoric water line.